Persistent Effects Induced by IL-13 in the Lung

Patricia C. Fulkerson, Christine A. Fischetti, Lynn M. Hassman, Nikolaos M. Nikolaidis, and Marc E. Rothenberg

Departments of Molecular Genetics, Biochemistry & Microbiology, and Cellular and Molecular Biology; and Division of Allergy and Immunology, Cincinnati Children's Hospital Medical Center, University of Cincinnati College of Medicine, Cincinnati, Ohio

IL-13 overexpression in the lung induces inflammatory and remodeling responses that are prominent features of asthma. Whereas most studies have concentrated on the development of IL-13–induced disease, far fewer studies have focused on the reversibility of IL-13–induced pathologies. This is particularly important because current asthma therapy appears to be poor at reversing lung remodeling. In this manuscript, we used an externally regulatable transgenic system that targets expression of IL-13 to the lung with the aim of characterizing the reversibility process. After 4 wk of doxycycline (dox) exposure, IL-13 expression resulted in mixed inflammatory cell infiltration, mucus cell metaplasia, lung fibrosis, and airspace enlargement (emphysema). After withdrawal of dox, IL-13 protein levels were profoundly reduced by 7 d and below baseline by 14 d. During this time frame, the level of lung eosinophils returned to near normal, whereas macrophages, lymphocytes, and neutrophils remained markedly elevated. IL-13–induced mucus cell metaplasia significantly decreased (91%) 3 wk after withdrawal of dox, showing strong correlation with reduced eosinophil levels. In contrast, IL-13–induced lung fibrosis did not significantly decline 4 wk after dox withdrawal. Importantly, IL-13–induced emphysema persisted, but modestly declined 4 wk after dox. Examination of transcript expression profiles identified a subset of genes that remained increased weeks after transgene expression was no longer detected. Notably, numerous IL-13–induced cytokines and enzymes were reversible (IL-6 and cathepsins), whereas others were sustained (CCL6 and chitinases) after IL-13 withdrawal, respectively. Thus, several hallmark features of IL-13–induced lung pathology persist and are dissociated from eosinophilia after IL-13 overexpression ceases.

Keywords: asthma; cytokines; eosinophils; inflammation; lung

Allergic asthma is characterized by chronic inflammation of the airways, airway wall remodeling, and a decline in respiratory function. In asthma, structural changes in the airway include mucus cell metaplasia, increased deposition of extracellular matrix proteins (e.g., collagen and proteoglycans), and hyperplasia of myofibroblasts and smooth muscle cells (1, 2). Airway remodeling and persistent inflammation contribute to disease pathogenesis of asthma. Animal studies have defined a critical effector role for IL-13 in many pathologic features of experimental asthma, including airway inflammation, tissue fibrosis, and mucus hypersecretion by goblet cells (3–5).

The effector functions mediated by IL-13 include a diverse array of biological activities (6). IL-13–deficient animals, novel IL-13 antagonists, and transgenic overexpression modeling systems have successfully defined a central role for IL-13 in some inflammatory diseases of the lung (6). In animal models, pulmonary overexpression of IL-13 results in inflammation, airway fibrosis, mucus metaplasia, airway hyperresponsiveness, and enhanced lung volumes and compliance (5, 7). The inflammatory response results, in part, from IL-13–induced chemokine and matrix metalloproteinase (MMP) expression and activity (8, 9). Chronic overexpression of IL-13 in the lung also results in alveolar remodeling through activation of proteolytic pathways by IL-13 (8, 9). While these studies identify pathways important in IL-13–induced inflammatory and remodeling responses, the natural history and reversibility of the remodeling response has not yet been adequately assessed.

Defining the reversibility of IL-13–induced tissue remodeling and pathology may have clinical significance, as tissue remodeling and fibrosis are important pathologic features of lung disease and do not appear to be clearly reversed by existing therapy (10–12). Airway remodeling has been proposed to result from repeated cycles of airway injury induced by inflammatory responses followed by processes inherent in the lung that repair the damaged airway (13). As asthma is a disease characterized by chronic inflammation and repeated inflammatory exacerbations, identification of critical pathways involved in the natural healing response in the injured airway could lead to the development of new therapies inhibiting the progression of the structural changes characteristic of these diseases. Collectively, these studies draw attention to the need to develop new therapeutic approaches to reverse and prevent airway structural changes.

In this study, we aimed to define the reversibility of chronic lung remodeling using an externally regulatable transgenic system that targets expression of IL-13 to the lung. Our studies demonstrate that while some aspects of chronic airway remodeling are reversible (e.g., mucus cell metaplasia and lung eosinophilia), other important features are primarily sustained during the repair process, providing compelling evidence that many of the prominent effects of IL-13 in the lung persist after the initial pathologic insult. Furthermore, to define the mechanism involved, we performed global transcript profile analysis and elucidate the genetic program associated with disease induction, remission, and persistence.

MATERIALS AND METHODS

Inducible IL-13 Lung Transgenic Mice

Bi-transgenic mice (CC10-iIL-13) were generated in which IL-13 was expressed in a lung-specific manner that allowed for external regulation of transgene expression, as previously described (14). Transgene expression was induced by feeding bi-transgenic mice doxycycline-impregnated (dox) food (625 mg/kg; Purina Mills, Richmond, IN). Animals were housed under pathogen-free conditions in accordance with institutional guidelines.

Bronchoalveolar Lavage Fluid Collection and Analysis

Mice were killed by an intraperitoneal injection of Ketaject (ketamine hydrochloride, 0.2 mg/kg; Phoenix Pharmaceuticals, St. Joseph, MO). A midline neck incision was made and the trachea was cannulated. The lungs were lavaged two times with 1.0 ml of lavage buffer (PBS containing 1% FCS). The recovered bronchoalveolar lavage fluid

(*Received in original form December 21, 2005 and in final form March 21, 2006*)

This work was supported in part by National Institutes of Health Grants R01 AI42242 (to M.E.R.), R01 AI45898 (to M.E.R.), and P01 HL-076383–01 (to M.E.R.).

Correspondence and requests for reprints should be addressed to Marc E. Rothenburg, Division of Allergy and Immunology, Cincinnati Children's Hospital Medical Center, University of Cincinnati College of Medicine, 3333 Burnet Avenue, Cincinnati, OH 45229-3039. E-mail: Rothenberg@cchmc.org

This article has an online supplement, which is accessible from this issue's table of contents at www.atsjournals.org

Am J Respir Cell Mol Biol Vol 35. pp 337–346, 2006
Originally Published in Press as DOI: 10.1165/rcmb.2005-0474OC on April 27, 2006
Internet address: www.atsjournals.org

(BALF) was centrifuged at 400 × *g* for 5 min at 4°C and resuspended in 200 μl of lavage buffer. Lysis of red blood cells was performed using RBC lysis buffer (Sigma, St. Louis, MO) according to the manufacturer's recommendations. Total cell numbers were counted with a hemacytometer. Cytospin preparations of 1×10^5 cells were stained with the Hema 3 Staining System (Fisher Diagnostics, Middletown, VA) and differential cell counts were determined.

Preparation of RNA and Microarray Hybridization

RNA was extracted using the TRIzol Reagent (Molecular Research Center, Inc., Cincinnati, OH) as per the manufacturer's instructions. After extraction, RNA was repurified with phenol-chloroform extraction and ethanol precipitation. Microarray hybridization to mouse expression array (MOE) 430 2.0 was performed by the Affymetrix Gene Chip Core facility at Cincinnati Children's Hospital Medical Center, as previously described (15). This analysis was performed with one mouse per chip ($n = 2$ for NO DOX [no transgene induction], $n = 3$ for DOX [4 wk of dox-induced IL-13 expression], and $n = 3$ DOX OFF [4 wk of dox-induced IL-13 expression followed by a 3-wk rest period]).

Northern Blot Analysis

RNA was electrophoresed in an agarose-formaldehyde gel, transferred to Gene Screen transfer membranes (NEN, Boston, MA) in 10× SSC (sodium chloride and sodium citrate) and cross-linked by ultraviolet radiation. The cDNA probes, generated by PCR or from commercially available vectors (I.M.A.G.E. Consortium obtained from American Tissue Culture Collection, Rockville, MD or Incyte Genomics, Palo Alto, CA), were sequence confirmed, radiolabeled with ^{32}P, and hybridized using standard conditions.

Microarray Data Analysis

Transcript expression differences between the groups (NO DOX [no transgene induction], DOX [4 wk of dox-induced IL-13 expression], and DOX OFF [4 wk of dox-induced IL-13 expression followed by a 3-wk rest period]) were determined using GeneSpring software (Silicon Genetics, Redwood City, CA). Data were normalized to the average of the NO DOX mice.

Eosinophil Quantitation

Lung tissue eosinophils were identified by anti–major basic protein (MBP) staining. The lungs were inflation-fixed in 10% neutral buffered formalin at 25 cm H_2O, embedded in paraffin, cut into 5-μm sections, and fixed to positively charged slides. Endogenous peroxidase in the tissues was quenched with 0.5% hydrogen peroxide in methanol. Lung sections were digested (10 min, 37°C) with pepsin (Zymed, San Francisco, CA), and blocked by incubation at room temperature in 3% normal goat serum in PBS for 2 h. The blocked sections were treated with rabbit anti-mouse MBP at 1:10,000 dilution (a kind gift of James and Nancy Lee, Mayo Clinic, Scottsdale, AZ) in 3% normal goat serum/PBS overnight at 4°C. The slides were subsequently washed free of primary antibody with several changes of PBS, followed by incubation with biotinylated goat anti-rabbit IgG (1:250 dilution) and avidin–peroxidase complex (Vector Laboratories, Burlingame, CA) for 2 h and 45 min, respectively. These slides were developed with nickel diaminobenzidine–cobalt chloride solution to form a black precipitate, and counterstained with nuclear fast red. Replacing the primary antibody with normal rabbit serum ablated the immunostaining. Quantification of immunoreactive cells was performed by counting the positive stained cells under low-power magnification of longitudinal sections, and eosinophil levels are expressed as the number of eosinophils per square millimeter.

Lung Histopathologic Changes

Mice were killed by an intraperitoneal injection of Ketaject (0.2 mg/kg; Phoenix Pharmaceuticals). Lungs were inflation-fixed with 10% neutral buffered formalin at 25 cm H_2O and immersed in the same fixative. The inflated lungs were embedded in paraffin, stained with either hematoxylin and eosin (H&E), periodic acid Schiff (PAS), or Masson's trichrome stain. PAS stained airway goblet cells were enumerated by light microscopy examination (×400 magnification). To quantitate the level of mucus expression in the airway, the number of PAS-positive and total epithelial cells in individual bronchioles was counted. At least three medium-sized bronchioles (defined by having ~ 90–150 luminal airway epithelial cells) were evaluated in each slide. Results are expressed as the percentage of PAS-positive cells per bronchiole, which is calculated from the number of PAS-positive epithelial cells per bronchiole divided by the total number of epithelial cells in each bronchiole.

Quantitation of BAL Mucin-5AC

To quantify levels of mucin-5AC (MUC-5AC) in BALF, serial dilutions (0.1 ml) of BALF were slot-blotted onto nytran membranes using the Minifold II slot blot apparatus (Schleicher and Schuell, Keene, NH) and allowed to air dry. After 2 h at room temperature in blocking buffer (1× PBS with 0.1% Tween-20 and 5% nonfat milk), the membrane was incubated with a monoclonal antibody against MUC-5AC (45M1; Neo Markers, Union City, CA) at room temperature for 1 h, washed three times in 1× PBS with 0.1% Tween-20, and then incubated with HRP-conjugated anti-mouse IgG #7076 (Cell Signaling Technology, Danvers, MA) at room temperature for 1 h. After three additional washes, immunoreactive MUC-5AC was detected using a chemiluminescent procedure (ECL Western Blotting Analysis System; Amersham Biosciences, Little Chalfont, Buckinghamshire, UK) and quantified by densitometry. Data are expressed as the mean of relative area of band size normalized to a standard area ($n = 3$ mice/group).

Lung Collagen Content

The left lung was homogenized in 2 ml of 0.5 M acetic acid. After the addition of pepsin (1 mg/10 mg tissue; Sigma), the lung homogenates were vigorously shaken overnight at 4°C. Collagen content was determined biochemically by quantifying total soluble collagen using the Sircol collagen assay kit (Biocolor Ltd, Newtownabbey, Northern Ireland, UK) according to the manufacturer's instructions. The data are expressed as the collagen content of the entire left lung.

Lung Homogenates

For cytokine quantitation, the right lung from CC10-iIL-13 mice was snap-frozen before or after transgene induction. The frozen lungs were homogenized in 0.4 ml of 50 mM Tris (pH 7.4). After addition of 0.4 ml of 0.1% Triton-X (Sigma), the lung homogenates were vortexed, incubated on ice for 15 min, then centrifuged at 13,000 × *g* for 15 min at 4°C.

ELISA Measurements

Cytokine levels were measured in BALF and lung homogenates using ELISA kits specific for IL-13, eotaxin-1, eotaxin-2, CXCL9 and IL-6 (R&D Systems, Minneapolis, MN), and TGFβ_1 (Promega Corporation, Madison, WI). The detection limits were 7, 10, 15, 12, 12, and 15 pg/ml for IL-6, eotaxin-1 and TGF-β_1, eotaxin-2, CXCL9 and IL-13, respectively.

Airspace Measurements

The overall proportion (% fractional area) of respiratory airspace was determined by using a point-counting method (16). Measurements were performed on sections taken from the left lobe. Slides were viewed using METAMORPH imaging software (Universal Imaging, West Chester, PA). A computer-generated, 100-point lattice grid was superimposed on each field and the number of intersections (points) falling over airspace was counted. Points falling over bronchioles, large vessels, and smaller arterioles and venules were excluded from the study. Fractional airspace area was calculated by dividing the number of points falling over airspace by the total number of points contained within the field and then multiplying by 100. Four fields per section were analyzed to gather the data. The *x* and *y* coordinates for each measured field were selected by using a random number generator.

RESULTS

Lung Resolution Model Using Externally Regulatable IL-13 Transgene Expression

To characterize the reversibility of IL-13–induced lung pathology, a transgenic overexpression system was developed to target

expression of IL-13 to the lung. An inducible dual-construct expression system was employed to externally regulate IL-13 expression in the lung (Figure 1A). At 5–6 wk of age, double-transgenic (CC10-iIL-13) mice were fed normal food pellets or dox food. Transgene mRNA was detectable by Northern blot analysis after 24 h on dox food and peaked within 1 wk (Figure 1B). After withdrawal of dox food, the IL-13 transgene was still detectable, but markedly reduced, after 7 d and was undetectable by 14 d (Figure 1B). In the absence of dox, BAL IL-13 protein levels were 29 ± 9 pg/ml (n = 4 experiments with three mice per experiment). In comparison, IL-13 protein levels in naïve nontransgenic mice were 48 ± 14 pg/ml (n = 8 mice). Increased (60-fold) levels of IL-13 protein expression were noted within 24 h of dox administration and peaked within 1 wk (107 ± 48 ng/ml; Figure 1C). IL-13 protein levels declined (95%) within 1 wk of dox withdrawal, and continued to decrease to baseline levels or below with time (Figure 1C). Together, these data demonstrate an expression system that involves externally regulatable and reversible exposure to the IL-13 in the lung.

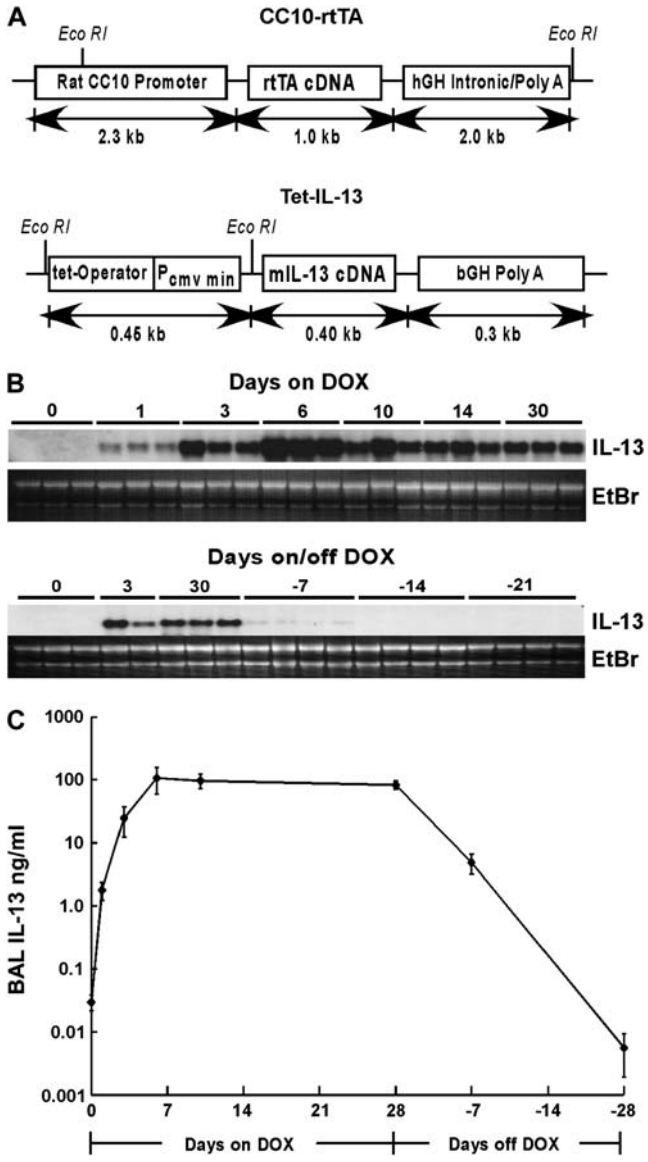

Figure 1. Inducible IL-13 expression in the lung. (*A*) Constructs used in the generation of CC10-iIL-13 mice. (B) Kinetics of IL-13 induction and cessation. Dual transgene positive mice were grown to adulthood on normal food pellets and then switched to dox-impregnated food. The levels of pulmonary IL-13 mRNA (*B*) were assessed at intervals before and after the addition of dox food. RNA was isolated from the lungs of CC10-iIL-13 mice fed dox-impregnated food for the indicated time periods. Each *lane* represents an individual mouse. In *C*, dual transgene positive mice received dox food for 28 d and then the dox food was removed. The levels of BALF IL-13 protein (*C*) were assessed at intervals before and after dox removal. Protein levels represent the mean ± SD of 4–6 mice at each time point.

Effects on Pulmonary Inflammation

To define the reversibility of IL-13–induced inflammation and tissue remodeling, we developed a resolution model that involved pulmonary IL-13 expression for 4 wk (DOX ON), followed by a 4-wk rest period (DOX OFF; Figure 2A). We first examined the effect of transgene regulation on the kinetics and resolution of IL-13–induced pulmonary inflammation. Dox-induced IL-13 expression resulted in inflammatory cell infiltration into the airway with increased macrophages, neutrophils, eosinophils and lymphocytes (Figures 2B–2D). Total BALF cells recovered from the airway increased 2-fold within 24 h of dox exposure (P = 0.005) and peaked (5–6 fold, P = 0.0004) after 4 wk of dox compared with control mice (Figure 2B). Interestingly, the marked cell accumulation (6-fold, P = 0.001) in the airways was sustained 14 d after dox withdrawal. Notably, after 4 wk on normal food, total inflammatory cell infiltration remained 2-fold greater than in control mice (Figure 2B). Macrophage infiltration significantly increased within 24 h of dox exposure (from 8 ± 1.5 × 10^4 to 16.9 ± 1.8 × 10^4, P = 0.006) and continued to increase over time with IL-13 expression (Figure 2C). After dox withdrawal, macrophage accumulation continued to increase, peaked 2 wk after dox withdrawal, then decreased after another 2 wk; however, this level was still higher than baseline (P = 0.002, Figure 2C). Neutrophil, eosinophil, and lymphocyte accumulation followed macrophage infiltration, significantly increasing after 6 d on dox food (1.1 ± 0.13 × 10^5 from 5.7 ± 2.3 × 10^3, 21 ± 4 × 10^3 from 1.5 ± 0.6 × 10^3, and 8.4 ± 1.2 × 10^3 from 1.9 ± 0.6 × 10^3, respectively; $P \leq 0.005$, Figures 2C and 2D). Similar to macrophages, BAL neutrophils and lymphocytes remained elevated 3 wk after dox withdrawal ($P \leq 0.006$, Figures 2C and 2D). After 4 wk on normal food, neutrophils remained increased (4-fold, P = 0.05) compared with control mice. In contrast, BAL eosinophilia dramatically decreased 1 wk after dox withdrawal, returning to baseline within 3 wk (Figure 2D).

Peribronchial and perivascular inflammatory cell accumulation is a prominent feature of pulmonary IL-13 overexpression; we therefore examined the reversibility of IL-13–induced lung tissue inflammation. IL-13 overexpression resulted in a marked increase in peribronchial and perivascular inflammatory cell accumulation when compared with control mice (Figure 3A). The inflammation was more pronounced surrounding the larger airways with inflammatory cells, especially eosinophils, surrounded by extracellular matrix (Figure 3B). Large, and occasionally multinucleated, airway macrophages contained granular and crystalline intracellular material (Figure 3C). Notably, significant inflammatory cells remained in the lung 3 wk after dox withdrawal (Figure 3D).

Recent studies have demonstrated a prominent role for IL-13 in allergen-induced eosinophil recruitment and have implicated eosinophils in allergen-induced airway remodeling (17–20). As such, we next investigated the kinetics of pulmonary eosinophilia in our resolution model. IL-13 expression resulted in eosinophil infiltration around bronchioles that increased over time; 10-fold within 10 d of dox exposure (P = 0.008) and 54-fold after 28 d

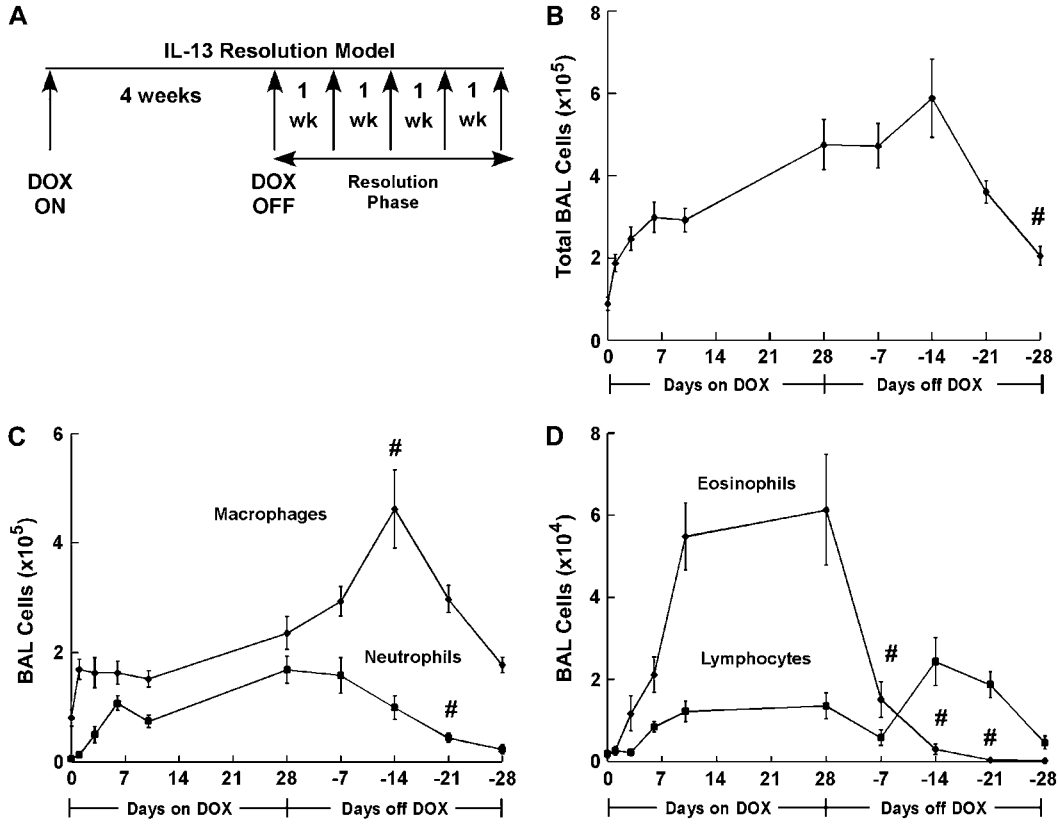

Figure 2. IL-13 transgene expression results in persistent airway inflammation. (*A*) A schematic representation of the IL-13 resolution model is depicted. Adult mice are fed dox-impregnated food for 4 wk and then given normal food. Multiple parameters are evaluated weekly after dox withdrawal (Resolution Phase). (*B*) Total BALF cells from CC10-iIL-13 mice fed dox-impregnated food (Days on DOX) and after dox withdrawal (Days off DOX) for the indicated days (n = 6–9 mice/group). All data points were statistically different ($P <$ 0.001) from non–dox-fed control mice after 1 d of dox administration. $^{\#}P = 0.003$ when compared with mice fed dox food for 28 d. (*C*) Macrophage and neutrophil composition of BALF from CC10-iIL-13 mice at indicated times in resolution model (n = 6–9 mice/group). All data points were statistically different ($P < 0.02$) than non–dox-fed mice after 1 d of dox administration for BAL macrophages and after 6 d for BAL neutrophils. $^{\#}P = 0.01$ when compared with mice fed dox-food for 28 d. (*D*) Eosinophil and lymphocyte composition of BALF from CC10-iIL-13 mice at indicated times in the resolution model (n = 6–9 mice/group). All points were significantly different ($P < 0.002$) from non–dox-fed control mice after 6 d of dox administration. $^{\#}P = 0.03$ when compared with mice fed dox food for 28 d.

($P < 0.001$, Figure 3E). Upon dox withdrawal, perivascular eosinophils were markedly reduced (75%, $P = 0.004$) within 7 d, and eosinophils surrounding the airways were reduced (80%, $P = 0.0004$) within 14 d (Figure 3E). Although perivascular eosinophils returned to baseline 4 wk after dox withdrawal, peribronchial eosinophils remained 3-fold higher than baseline ($P =$ 0.04, Figures 3E and 3F). We next examined the kinetics of expression of the eosinophil-specific eotaxin chemokines in the BALF of CC10-iIL-13 mice. Protein levels of eotaxin-1 and eotaxin-2 were increased within 10 d of IL-13 transgene expression and peaked after 4 wk of dox administration (Figure 3G). Peak induction of eotaxin-2 (277-fold) was greater than eotaxin-1 (16-fold) after 4 wk of IL-13 transgene expression, but both chemokines returned to baseline within 2 wk after dox withdrawal (Figure 3G). Taken together, IL-13 initiated a sustained airway and tissue inflammation involving macrophages, neutrophils, and lymphocytes, whereas IL-13–induced eosinophilia more rapidly declined after dox withdrawal correlating with decreased expression of the eotaxin chemokines in the lung.

Effects on Lung Remodeling

A wealth of studies have described a critical role for IL-13 in lung remodeling including mucus cell metaplasia, mucus overproduction and emphysema (6). To define the reversibility of IL-13–induced mucus production, we examined PAS-positive cells in the bronchial epithelium at different time points in our resolution model. IL-13 expression resulted in a prominent increase in mucus production (37 ± 14% of airway epithelium was PAS-positive) within 3 d and peaked within 6–10 d (60 ± 2%; Figures 4A and 4B). After 4 wk of IL-13 expression, PAS^+ epithelium decreased (28 ± 1% versus 60 ± 2%, $P < 0.0001$) and continued to decline upon withdrawal of dox and decrease in transgene expression (Figures 4A and 4B). Importantly, mucus production remained present, although markedly reduced, in the lungs 3 wk after dox withdrawal. At all time points, PAS-stained cells could not be appreciated, or were extremely rare, in the airways of control CC10-iIL-13 (NO DOX) mice (data not shown). We also examined the kinetics of mucus secretion in our resolution model. Four weeks of IL-13 expression resulted in significantly increased mucin secretion into BAL fluid compared with control NO DOX mice as assessed by immunoblot analysis (18 ± 3 versus 50 ± 10.8 relative area, $P < 0.008$), whereas no significant increase was observed 6 and 10 d after dox exposure (data not shown). Mucin secretion decreased 2 and 4 wk after dox withdrawal, but not to baseline levels (data not shown).

We next investigated the reversibility of IL-13–induced lung fibrosis. Total collagen content in one lobe of the lung was measured based on the specific binding of collagen to the dye Sirius Red. Total collagen content of the lung was significantly increased (3.6 ± 1.8 fold, $n = 3$ experiments) after 4 wk of IL-13 expression (Figure 5A). There was no significant difference in collagen content between wild-type mice fed dox food and control CC10-iIL-13 mice fed normal food (459 ± 116 versus 452 ± 73 μg/left lobe, respectively, $n = 4$ mice/group). Total lung collagen did not significantly change 4 wk after dox withdrawal (Figure 5A). We also examined the distribution of collagen deposition by Masson's trichrome staining. Enhanced collagen deposition was readily apparent in the subepithelial regions of airways within 6 d of IL-13 transgene induction (Figure 5B). This

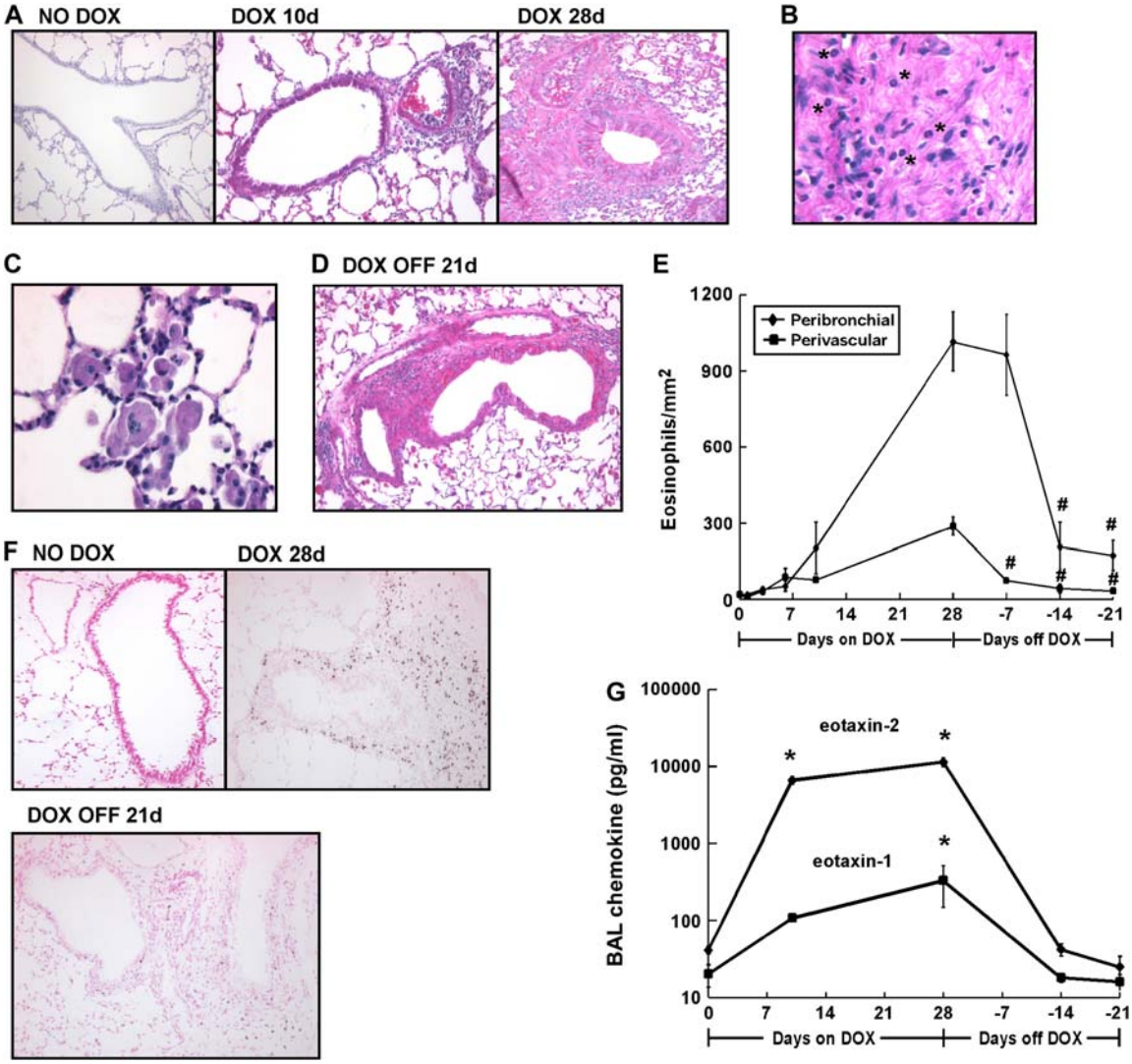

Figure 3. IL-13 transgene expression results in sustained tissue inflammation. (*A*) H&E-stained lungs from CC10-iIL-13 mice fed normal (NO DOX) or dox-food (DOX) for the indicated times are shown. (*B*) Infiltrating leukocytes trapped in extracellular matrix are shown. *Eosinophils. (*C*) Enlarged macrophages within the airspace are shown. (*D*) Inflammation surrounding blood vessels and airways 3 wk after dox withdrawal (DOX OFF) is shown. (*E*) Kinetics of IL-13–induced eosinophil infiltration around blood vessels (perivascular, *squares*) and bronchioles (peribronchial, *diamonds*) is shown (n = 4–11 mice/group). All points were significantly different ($P < 0.05$) from non–dox-fed control mice after 10 d of dox administration. $^{\#}P \leq 0.004$ when compared with mice fed dox food for 28 d. (*F*) Eosinophils, detected by anti-MBP immunohistochemistry, are shown in lung tissue at different time points within the resolution model. (*G*) Eotaxin-1 and eotaxin-2 protein levels in the BALF of CC10-iIL-13 mice fed normal (NO DOX) or dox-food (DOX) for the indicated time are shown. Protein levels represent mean ± SD of 4–7 mice at each time point. $^{*}P < 0.0001$ when compared with non–dox-fed control mice. Magnification in *A–D*, *F*: ×100–400.

accumulation was most prominent in the larger airways, but was evident in the smaller airways with longer IL-13 exposure (Figure 5B). Examination of lungs after dox withdrawal revealed little or no change in collagen deposition around larger airways (Figure 5B).

As TGF-β_1 has been implicated as a critical mediator of IL-13–induced fibrosis (21), we measured total TGF-β_1 protein levels in BAL fluids collected at different time points in our resolution model. Significantly increased TGF-β_1 levels were detected within 6 d of IL-13 expression ($P = 0.01$) and continued to increase over time (Figure 5C). Two weeks after dox withdrawal, TGF-β_1 levels were markedly reduced, but remained significantly increased compared with controls ($P = 0.002$, Figure 5C).

Abnormally large airspaces are a characteristic feature of emphysema and have been associated with IL-13 overexpression (5, 9, 22). To determine if IL-13–induced airspace enlargement can be reversed, we measured the percentage of fractional airspace in the lungs of CC10-iIL-13 mice. Within 4 wk of transgene expression, the fractional area of airspace was significantly ($P < 0.0001$) increased compared with control mice (Figures 6A and 6B). After dox withdrawal, there was a modest, but significant, decrease in percentage of fractional area of airspace with persistence of airspace enlargement (Figures 6A and 6B). Taken together, these data reveal that several of the hallmark features of IL-13–induced pathology in the lung primarily persist after IL-13 overexpression ceases.

Effects on Gene Transcription

To gain insight into molecular mechanisms critically involved in IL-13–induced lung remodeling and the repair processes that

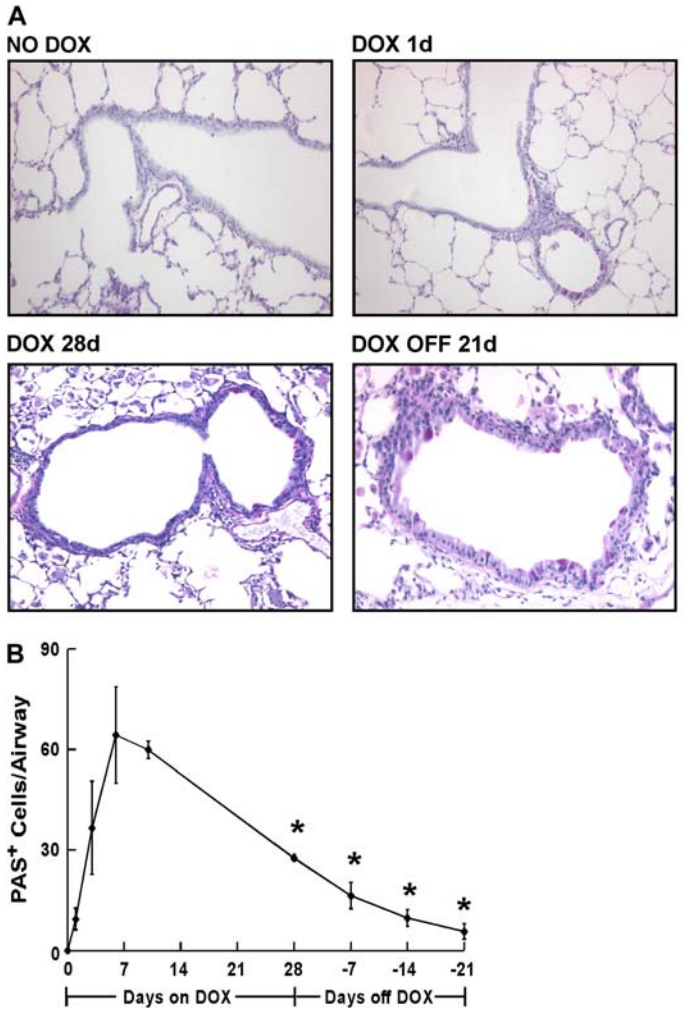

Figure 4. Resolution of IL-13–induced mucus production. (*A*) Kinetics of mucus induction and resolution as shown in PAS-stained lungs from CC10-rtTA-IL-13 mice fed normal (NO DOX) or dox food (DOX) for the indicated times. Magnification: ×100. (*B*) Quantitation of PAS^+ cells (mean ± SD) in airways of CC10-rtTA-IL-13 mice at indicated times in the resolution model (n = 4–6 mice/group). *$P < 0.001$ when compared with 10 d of dox administration.

follow, we analyzed global gene expression profiles at two different time points in our resolution model: after 4 wk of dox-induced IL-13 expression (DOX) and 3 wk after dox withdrawal (DOX OFF; Figure 7A). IL-13 expression in the lung for 4 wk was a potent inducer of gene expression, resulting in 743 genes, or 5.3% of the mouse genome, induced 2-fold or more compared with control lungs with no transgene induction (Figure 7B). Three weeks after dox withdrawal, 101 genes were induced ⩾ 2-fold (Figure 7B). Of the IL-13–induced genes, 10% (77 of 743) remained induced ⩾ 2-fold 3 wk after dox withdrawal (Figure 7B). Twenty-four new genes were induced ⩾ 2-fold during the resolution phase that were not induced during DOX (IL-13 transgene expression); most of these new genes were ESTs (Figure 7B and data not shown). The complete list of genes induced 2-fold or more in the DOX and DOX OFF groups can be found in Tables E1 and E2 in the online supplement, respectively. Cytokines and cytokine receptors represented a large subset of genes induced by IL-13 expression (Table 1). Sixteen chemokines (10 CC and 6 CXC chemokines), members of the IL-1 family (IL-1α, IL-1β, and IL1R antagonist), IL-6, IL-10Rα, and IL-13Rα2 were among the IL-13–induced genes (Table 1). Notably, CCL6, CCL8, and CXCL1 remained induced 3 wk after dox withdrawal, suggesting that these chemokines may contribute to the sustained pulmonary inflammation in the absence of transgene expression. The remaining cytokines and receptors returned to near baseline after 3 wk off dox. In accordance with the microarray data, dox-induced IL-13 expression resulted in increased BALF IL-6 from 18.8 ± 2.9 to 51.3 ± 6.0 pg/ml (mean ± SEM, n = 6 mice per group) after 4 wk, but decreased to below the level of detection (< 7 pg/ml) 2 wk after dox withdrawal. Also, consistent with the IL-13–induced expression of CXCL9 mRNA, analysis of protein levels revealed an increase in CXCL9 in lung homogenates after 4 wk of IL-13 expression, from 253 ± 29 to 1,020 ± 92 pg/ml (mean ± SD, n = 4–5 mice per group). Sustained induction of the chemokines CCL6 and CXCL5 3 wk after dox withdrawal was observed by Northern blot analysis (Figure 7C). Expression of these potent macrophage and neutrophil chemoattractants in the lung is consistent with their contributory role in maintaining lung inflammation in the absence of IL-13 expression. In contrast, CXCL5 and CXCL10 were induced with IL-13 expression, but were no longer detectable by Northern blot analysis 3 wk after dox withdrawal (Figure 7B).

IL-13 also induced several genes coding for proteases and enzymes associated with inflammation and remodeling, including MMPs, cathepsins, and chitinases (5, 9, 23) (Table 2). Importantly, proteases were among those genes that remained induced after dox withdrawal, consistent with a contributory role for these proteins in the repair process in the lung. Genes encoding transporter proteins, including glucose, zinc and amino acid transporters, and a number of different calcium-activated chloride channels, were induced with IL-13 expression (Table 2). Interestingly, Clca4, a calcium-activated chloride channel expressed by smooth muscle cells, was induced only in the DOX OFF group. These results identify a subset of genes that are

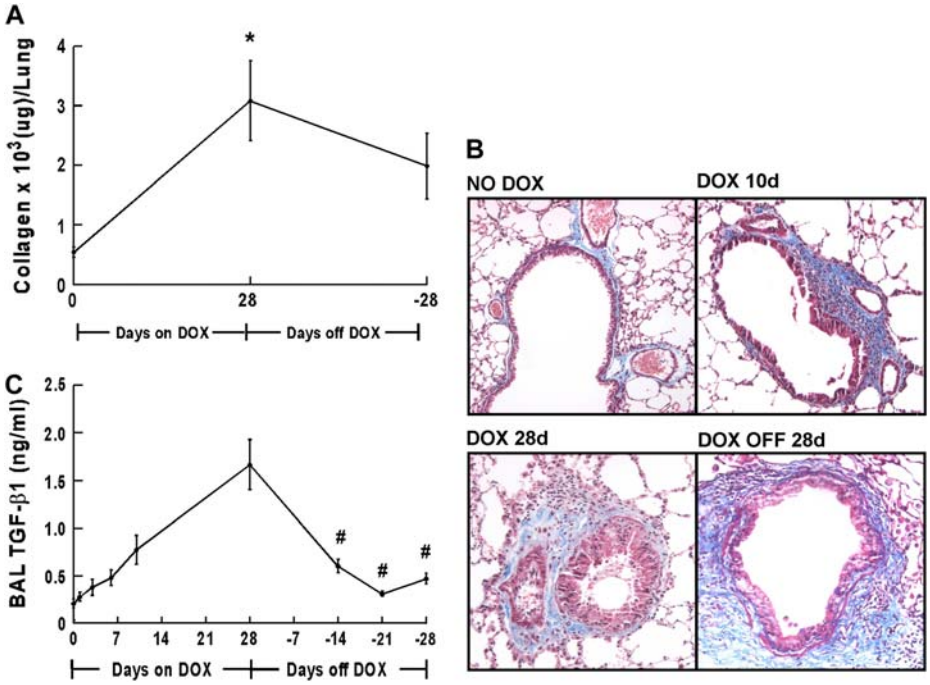

Figure 5. Persistence of IL-13–induced collagen deposition. (*A*) Collagen content of the left lobe of CC10-rIL-13 mice using Sircol assay at indicated times in resolution model is shown ($n = 2$ experiments with a representative experiment shown). $^{*}P \leq 0.003$ when compared with non–dox-fed control mice. (*B*) Localization of collagen in CC10-rIL-13 mice over time as shown by Masson's trichrome staining. (*C*) Levels of active TGF-β_1 in BALF from CC10-rIL-13 mice at indicated times in resolution model are shown (4–8 mice/group). $^{\#}P \leq 0.03$ when compared with mice fed dox food for 28 d.

induced in the lung with chronic IL-13 exposure and remained induced for weeks after cessation of IL-13 expression.

DISCUSSION

Allergic asthma is a chronic inflammatory disease characterized by recurrent episodes of airway obstruction and wheezing. In susceptible individuals, intermittent exposure to allergens results in a complex inflammatory response, leading to airway injury and chronic lung inflammation. The recurrent inflammatory exacerbations, along with persistent local inflammation, induce cycles of injury and repair that likely induce airway remodeling, structural changes in the airway wall that contribute to disease pathogenesis and possible progression to emphysema. Although a wealth of studies have characterized mediators implicated in airway wall remodeling, the natural history of the inflammatory response and the reversibility of the remodeled airway remains under-investigated. In this study, we aimed to define the

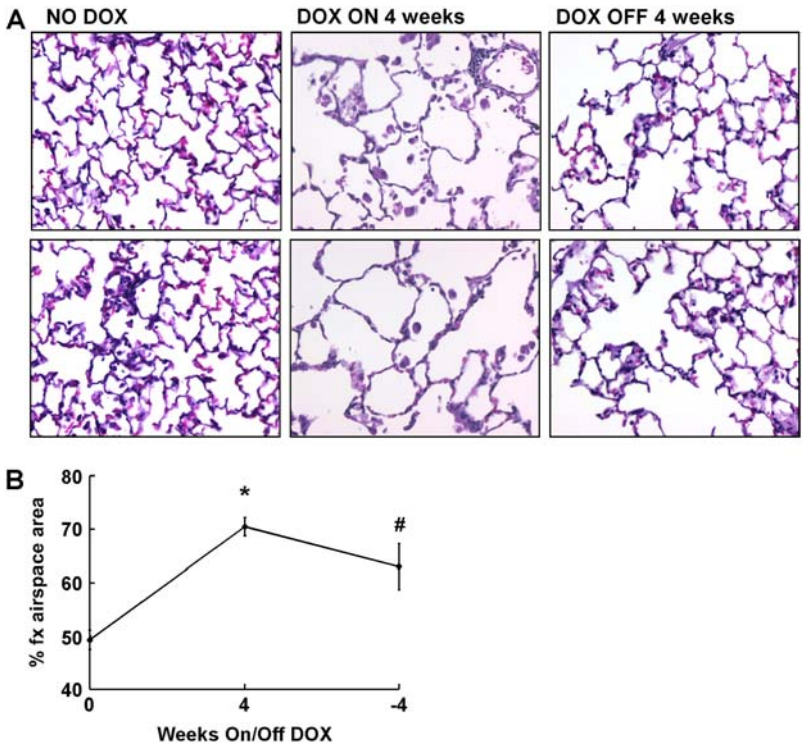

Figure 6. Persistence of IL-13–induced emphysema. (*A*) Induction of airspace enlargement as shown in H&E stained lungs from CC10-rIL-13 mice fed normal (NO DOX) or dox food (DOX) for the indicated number of weeks. Each *panel* is an individual mouse. Magnification: ×200. (*B*) Quantitation of percentage of fractional area of airspace (% fx airspace area) of CC10-rIL-13 mice at indicated times in the resolution model ($n = 2$ experiments, with 4–8 mice/group/experiment). A representative experiment is shown. $^{*}P < 0.0001$ when compared with non–dox-fed control mice. $^{\#}P = 0.002$ when compared with mice fed dox food for 28 d.

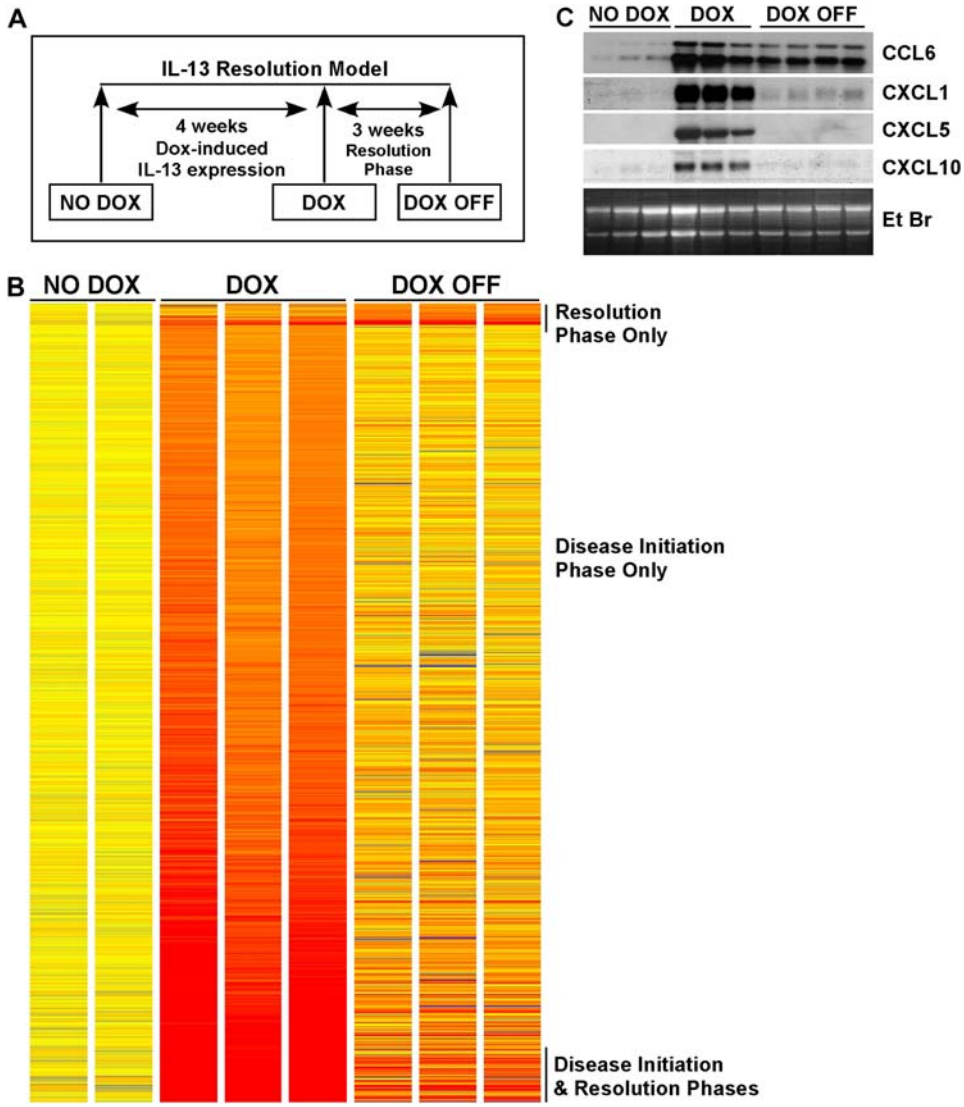

Figure 7. Identification of IL-13–induced genes. (*A*) A schematic diagram of the IL-13 resolution model is depicted, indicating the three time points of analysis: before transgene induction (NO DOX), 4 wk with transgene expression (DOX), and 3 wk after transgene turned off (DOX OFF). (*B*) The 767 genes differentially expressed ($P < 0.05$) in the lungs of CC10-iIL-13 mice at indicated time points in the model compared with NO DOX control mice are shown; upregulated genes are represented in *red* and downregulated genes in *blue*. The magnitude of the gene changes is proportional to the darkness of the color. Each *column* represents an individual mouse and each line a gene. (*C*) Northern blot analysis confirmed sustained induction of CCL6 and CXCL1, but not CXCL5 or CXCL10 by IL-13 transgene expression. The ethidium bromide (EtBr)-stained gel is shown. Each *lane* represents an individual mouse.

reversibility of IL-13–induced chronic inflammation and lung remodeling. As such, we developed a disease progression and resolution model using an externally regulatable transgenic system that targets expression of IL-13 to the lung. First, we demonstrate that the inflammatory infiltrate, composed primarily of macrophages, neutrophils, and lymphocytes, persists in the lung 3–4 wk after IL-13 expression ceases. Second, we demonstrate that while IL-13 rapidly induces mucus cell metaplasia, there is a significant decline in the number of mucus-producing cells during the initiation phase (dox exposure) that correlates with a significant increase in mucin secretion into the BAL fluid, suggesting that signals that promote mucus secretion are kinetically distinct from signals that induce mucus production. Third, we demonstrate that IL-13–induced mucus cell metaplasia and lung eosinophilia are highly dependent on IL-13 production, as a reduction in the severity of both parameters strongly correlates with decreasing IL-13 protein levels. Fourth, we demonstrate that airspace enlargement only modestly improves after IL-13 decline (dox withdrawal). And finally, we identify the genetic program (transcript profile) associated with disease initiation and resolution. Notably, a subset of the initiation genes remain elevated during the resolution phase. These sustained genes, including multiple chemokines, proteases, enzymes, and transporters, are likely involved in regulating the inflammatory response and airway remodeling initially stimulated by IL-13. In addition, we define a set of 24 genes that are only induced during the resolution phase of IL-13–associated lung injury.

Leukocyte recruitment into the lung has been shown to be partially dependent on chemokines in IL-13 overexpression models (8, 24). In particular, IL-13 has been shown to be a potent inducer of a number of CC chemokines (8). In our study, we demonstrate IL-13–induced expression of chemokines from both the CC and CXC families (Table 1). We also identify a subset of chemokines, including CCL6, CCL8, and CXCL1, which are induced with chronic IL-13 exposure (4 wk) and remained induced after cessation of IL-13 expression, suggesting a contributory role in the persistent lung inflammation. Although Northern blot analysis showed CCL6 expression diminished very little over time and CXCL1 expression dropped considerably more, it is important to note that both chemokines remained increased after dox withdrawal compared with non-induced transgenic mice (Figure 6C). Previous studies have implicated a role for CCL6 in regulating IL-13–induced inflammation (24).

Surprisingly, chronic IL-13 expression resulted in expression of the Th1-associated chemokines, CXCL9 and CXCL10. Expression of these chemokines in experimental asthma has been

TABLE 1. CYTOKINES AND RECEPTORS INDUCED 2-FOLD OR MORE IN IL-13–INDUCED RESOLUTION MODEL*

Common Gene Name	GenBank	DOX	DOX OFF
CCL2, JE	AF065933	+	−
CCL3, Mip-1α	NM_011337	+	−
CCL4, MIP-1β	AF128218	+	−
CCL7, MCP-3	AF128193	+	−
CCL9, MRP-2	AF128196	+	−
CCL11, eotaxin-1	NM_011330	+	−
CCL12, MCP-5	U50712	+	−
CCL24, eotaxin-2	AF281075	+	−
CXCL2, Gro-β	NM_009140	+	−
CXCL5, LIX	NM_009141	+	−
CXCL9, Mig	NM_008599	+	−
CXCL10, IP-10	NM_021274	+	−
CXCL12, SDF-1	BC006640	+	−
CCR1	AV231648	+	−
CCR5	D83648	+	−
IL-1β	BC011437	+	−
IL-6	NM_031168	+	−
IL-10Rα	NM_008348	+	−
IL-13Rα2	BC003723	+	−
IL-7 receptor	AI573431	+	−
IL-1 receptor antagonist	NM_031167	+	−
CCL6, C10	**BC002073**	**+**	**+**
CCL8, MCP-2	**NM_021443**	**+**	**+**
CXCL1, KC	**NM_008176**	**+**	**+**
CCR9	**BB124954**	**+**	**+**
CXCR6	NM_030712	−	+

Definition of abbreviations: DOX, mice fed doxycycline; DOX OFF, mice after 3 wk of doxycycline withdrawal.

* If expression of the gene is induced at least ⩾ 2-fold compared with NO DOX controls, the gene is labeled with "+." If transcript levels of the gene do not increase at least 2-fold, the gene is labeled with "−." Genes induced ⩾ 2-fold in both groups are shown in bold type.

TABLE 2. GENES INDUCED 2-FOLD OR MORE IN IL-13–INDUCED RESOLUTION MODEL*

Common Gene Name	GenBank	DOX	DOX OFF
Arginase I	NM_007482	+	−
Arginase II	NM_009705	+	−
Ear11	BC020070	+	−
MMP12	BC019135	+	−
MMP13	NM_008607	+	−
Adam8	NM_007403	+	−
Cathepsin B	BG067383	+	−
Cathepsin S	NM_021281	+	−
Cathepsin Z	NM_022325	+	−
Dipeptidylpeptidase 7	BB746075	+	−
Hexoaminidase A	U07631	+	−
Hexoaminidase B	NM_010422	+	−
Timp1	BC008107	+	−
Serpina3g	BC002065	+	−
Serpinb2	NM_011111	+	−
GLUT1 (Slc2a1)	BM207588	+	−
CAT2 (Slc7a2)	BF533509	+	−
Sglt1 (Slc5a1)	AF208031	+	−
cl-1 (Slc15a3)	NM_023044	+	−
Nramp-1 (Slc11a1)	NM_013612	+	−
C1q-β	AW227993	+	−
Complement component factor i	NM_007686	+	−
Inhibin-βa	NM_008380	+	−
Sprr-2a	NM_011468	+	−
Elastin	BB229377	+	−
Macrophage scavenger receptor 1	BC003814	+	−
Lipocalin 2	X14607	+	−
Complement component 3a receptor 1	NM_009779	+	−
G protein–coupled receptor 35	NM_022320	+	−
G protein–coupled receptor 43	AV370830	+	−
G protein–coupled receptor 65	NM_008152	+	−
Trem1	BB784999	+	−
Trem2	NM_031254	+	−
Toll-like receptor 8	NM_133212	+	−
Toll-like receptor 7	**AY035889**	**+**	**+**
MMP19	**AF153199**	**+**	**+**
Ym2 (Chi3l3)	**NM_009892**	**+**	**+**
Brp39 (Chi3l1)	**BC005611**	**+**	**+**
Cathepsin K	**NM_007802**	**+**	**+**
Slc39a2	**BB049001**	**+**	**+**
Slc26a4	**NM_011867**	**+**	**+**
Mucolipin 3	**NM_134160**	**+**	**+**
Clca1	**AF108501**	**+**	**+**
Clca4	AY008277	−	+
HSP105	B1499717	−	+

Definition of abbreviations: DOX, mice fed doxycycline; DOX OFF, mice after 3 wk of doxycycline withdrawal.

* If expression of the gene is induced at least ⩾ 2-fold compared with NO DOX controls, the gene is labeled with "+." If transcript levels of the gene do not increase at least 2-fold, the gene is labeled with "−." Genes induced ⩾ 2-fold in both groups are shown in bold type.

shown to be dependent on IFN-γ and the transcription factor Stat1 (25). In an experimental model using intratracheal delivery of cytokines, IL-4, but not IL-13, induced IFN-γ expression (26). Consistent with this, IFN-γ levels remain relatively unchanged throughout our resolution model (data not shown), suggesting an alternative mechanism induced by chronic IL-13 expression for induction or accumulation of CXCL9 and CXCL10 mRNA. Proteases and enzymes, such as MMPs, cathepsins, and chitinases, have also been shown to regulate IL-13–induced inflammation and remodeling (5, 9, 23). Our results, demonstrating markedly sustained induction of chemokines and proteases, suggest that these genes also likely contribute to the persistent airway infiltrate and support a role for these chemoattractants and proteases in the perpetuation and exacerbation of IL-13–induced airway remodeling.

Asthma and COPD are obstructive pulmonary disorders involving chronic airway inflammation. Asthma has long been considered as a condition of reversible airflow obstruction; however, many individuals with asthma have residual airflow obstruction (27). Irreversible airflow obstruction seen primarily in individuals with severe asthma may be due to persistent underlying bronchial inflammation and airway remodeling. Although IL-13–induced lung fibrosis did not significantly change 4 wk after dox withdrawal, there was a modest decline observed. Further studies are needed to determine if the collagen content would decrease further at later time points. COPD is also characterized by airflow limitations that are not fully reversible. One of the major mechanisms of airway obstruction in COPD is loss of alveolar walls due to proteolytic destruction of the lung parenchyma. Reversal of this process by drug therapy has remained elusive, although retinoic acid has been shown to increase the number of alveoli in a rat experimental emphysema model (28, 29). In our model, IL-13–induced airspace enlargement mainly persists in the absence of transgene expression, suggesting a mechanism in the inherent healing process for restoration for some lost alveolar tissue, despite protease expression that remains elevated after dox withdrawal. While current and proposed treatments for emphysema are aimed at preventing or modifying future remodeling (30), identification of pathways important in the repair of the damaged lung could lead to novel therapeutics directed toward alveolar restoration. It is hopeful that the identified gene transcript profiles that correlate with emphysema may be helpful in this regard. Further studies are needed to determine if an increase in the repair of the alveoli structure results in improved lung function.

In our model, macrophage infiltration continued to increase, while mucus cell metaplasia and lung eosinophilia declined in the absence of IL-13 expression. In addition, expression of a subset of IL-13–induced genes remained increased weeks after transgene expression was no longer detected. Thus, chronic exposure to IL-13 in the lung induced a long-lived pathologic and genetic response that was observed in the absence of IL-13. Understanding the mechanisms that contribute to persistent inflammation and airway wall remodeling could lead to the identification of new therapeutic targets. Our findings implicate proteases (e.g., MMPs, cathepsins, and chitinases) as potential targets against which therapies can be directed in the treatment of diseases associated with lung remodeling. In addition, genes that remain induced during the resting phase are potentially beneficial to the continued resolution of the IL-13–induced lung pathology. As such, the identified candidate genes offer several new mechanistic approaches to better understand the injury and repair cycle of chronic lung disease associated with Th2 immunity.

Conflict of Interest Statement: P.C.F. does not have a financial relationship with a commercial entity that has an interest in the subject of this manuscript. C.A.F. does not have a financial relationship with a commercial entity that has an interest in the subject of this manuscript. L.M.H. does not have a financial relationship with a commercial entity that has an interest in the subject of this manuscript. N.M.N. does not have a financial relationship with a commercial entity that has an interest in the subject of this manuscript. M.E.R. has participated as part of the Merck Speaker's Bureau and has received honoraria for this (~$30,000 over the last three years). He received $10,000 in 2002+ for serving as a consultant for Cambridge Antibody Technology and a $45,000 grant from this company to conduct another study. He has been a consultant for Ception Therapeutics for the past two years and has received stock ($37,000). He has been a consultant for GlaxoSmithKline for the past five years and has received ~$10,000. He has received a $2000 honorarium from Tanox Inc. Finally, he received two unrestricted Visiting Professorship awards from Pfizer ($7500 each) in 2003 and 2005.

***Acknowledgments*:** The authors thank Dr. Fred Finkelman for helpful discussions and review of this manuscript; Drs. Jeff Whitsett and Jamie and Nancy Lee for critical reagents; Dr. Susan Wert for advice and technical assistance with the emphysema measurement; and Andrea Lippelman for assistance with the preparation of this manuscript.

References

1. Elias JA, Zhu Z, Chupp G, Homer RJ. Airway remodeling in asthma. *J Clin Invest* 1999;104:1001–1006.
2. Bousquet J, Chanez P, Lacoste JY, White R, Vic P, Godard P, Michel FB. Asthma: a disease remodeling the airways. *Allergy* 1992;47:3–11.
3. Wills-Karp M, Luyimbazi J, Xu X, Schofield B, Neben TY, Karp CL, Donaldson DD. Interleukin-13: central mediator of allergic asthma. *Science* 1998;282:2258–2261.
4. Kuperman DA, Huang X, Koth LL, Chang GH, Dolganov GM, Zhu Z, Elias JA, Sheppard D, Erle DJ. Direct effects of interleukin-13 on epithelial cells cause airway hyperreactivity and mucus overproduction in asthma. *Nat Med* 2002;8:885–889.
5. Zheng T, Zhu Z, Wang Z, Homer RJ, Ma B, Riese RJ Jr, Chapman HA Jr, Shapiro SD, Elias JA. Inducible targeting of IL-13 to the adult lung causes matrix metalloproteinase- and cathepsin-dependent emphysema. *J Clin Invest* 2000;106:1081–1093.
6. Wynn TA. IL-13 effector functions. *Annu Rev Immunol* 2003;21:425–456.
7. Zhu Z, Homer RJ, Wang Z, Chen Q, Geba GP, Wang J, Zhang Y, Elias JA. Pulmonary expression of interleukin-13 causes inflammation, mucus hypersecretion, subepithelial fibrosis, physiologic abnormalities, and eotaxin production. *J Clin Invest* 1999;103:779–788.
8. Zhu Z, Ma B, Zheng T, Homer RJ, Lee CG, Charo IF, Noble P, Elias JA. IL-13-induced chemokine responses in the lung: role of CCR2 in the pathogenesis of IL-13-induced inflammation and remodeling. *J Immunol* 2002;168:2953–2962.
9. Lanone S, Zheng T, Zhu Z, Liu W, Lee CG, Ma B, Chen Q, Homer RJ, Wang J, Rabach LA, *et al.* Overlapping and enzyme-specific contributions of matrix metalloproteinases-9 and -12 in IL-13-induced inflammation and remodeling. *J Clin Invest* 2002;110:463–474.
10. Suissa S, Ernst P. Inhaled corticosteroids: impact on asthma morbidity and mortality. *J Allergy Clin Immunol* 2001;107:937–944.
11. Doherty DE. The pathophysiology of airway dysfunction. *Am J Med* 2004;117:11S–23S.
12. Man SF, Sin DD. Inhaled corticosteroids in chronic obstructive pulmonary disease: is there a clinical benefit? *Drugs* 2005;65:579–591.
13. Busse W, Elias J, Sheppard D, Banks-Schlegel S. Airway remodeling and repair. *Am J Respir Crit Care Med* 1999;160:1035–1042.
14. Wan H, Kaestner KH, Ang SL, Ikegami M, Finkelman FD, Stahlman MT, Fulkerson PC, Rothenberg ME, Whitsett JA. Foxa2 regulates alveolarization and goblet cell hyperplasia. *Development* 2004;131:953–964.
15. Zimmermann N, Mishra A, King NE, Fulkerson PC, Doepker MP, Nikolaidis NM, Kindinger LE, Moulton EA, Aronow BJ, Rothenberg ME. Transcript signatures in experimental asthma: identification of STAT6-dependent and -independent pathways. *J Immunol* 2004;172:1815–1824.
16. Wert SE, Yoshida M, LeVine AM, Ikegami M, Jones T, Ross GF, Fisher JH, Korfhagen TR, Whitsett JA. Increased metalloproteinase activity, oxidant production, and emphysema in surfactant protein D gene-inactivated mice. *Proc Natl Acad Sci USA* 2000;97:5972–5977.
17. Cho JY, Miller M, Baek KJ, Han JW, Nayar J, Lee SY, McElwain K, McElwain S, Friedman S, Broide DH. Inhibition of airway remodeling in IL-5-deficient mice. *J Clin Invest* 2004;113:551–560.
18. Humbles AA, Lloyd CM, McMillan SJ, Friend DS, Xanthou G, McKenna EE, Ghiran S, Gerard NP, Yu C, Orkin SH, *et al.* A critical role for eosinophils in allergic airways remodeling. *Science* 2004;305:1776–1779.
19. Lee JJ, Dimina D, Macias MP, Ochkur SI, McGarry MP, O'Neill KR, Protheroe C, Pero R, Nguyen T, Cormier SA, *et al.* Defining a link with asthma in mice congenitally deficient in eosinophils. *Science* 2004;305:1773–1776.
20. Pope SM, Brandt EB, Mishra A, Hogan SP, Zimmermann N, Matthaei KI, Foster PS, Rothenberg ME. IL-13 induces eosinophil recruitment into the lung by an IL-5- and eotaxin-dependent mechanism. *J Allergy Clin Immunol* 2001;108:594–601.
21. Lee CG, Homer RJ, Zhu Z, Lanone S, Wang X, Koteliansky V, Shipley JM, Gotwals P, Noble P, Chen Q, *et al.* Interleukin-13 induces tissue fibrosis by selectively stimulating and activating transforming growth factor beta(1). *J Exp Med* 2001;194:809–821.
22. Blundell R, Harrison DJ, Wallace WA. Emphysema: the challenge of the remodelled lung. *J Pathol* 2004;202:141–144.
23. Zhu Z, Zheng T, Homer RJ, Kim YK, Chen NY, Cohn L, Hamid Q, Elias JA. Acidic mammalian chitinase in asthmatic Th2 inflammation and IL-13 pathway activation. *Science* 2004;304:1678–1682.
24. Ma B, Zhu Z, Homer RJ, Gerard C, Strieter R, Elias JA. The C10/CCL6 chemokine and CCR1 play critical roles in the pathogenesis of IL-13-induced inflammation and remodeling. *J Immunol* 2004;172:1872–1881.
25. Fulkerson PC, Zimmermann N, Hassman LM, Finkelman FD, Rothenberg ME. Pulmonary chemokine expression is coordinately regulated by STAT1, STAT6, and IFN-gamma. *J Immunol* 2004;173:7565–7574.
26. Finkelman FD, Yang M, Perkins C, Schleifer K, Sproles A, Santeliz J, Bernstein JA, Rothenberg ME, Morris SC, Wills-Karp M. Suppressive effect of IL-4 on IL-13-induced genes in mouse lung. *J Immunol* 2005;174:4630–4638.
27. Gelb AF, Zamel N. Unsuspected pseudophysiologic emphysema in chronic persistent asthma. *Am J Respir Crit Care Med* 2000;162:1778–1782.
28. Massaro GD, Massaro D. Retinoic acid treatment abrogates elastase-induced pulmonary emphysema in rats. *Nat Med* 1997;3:675–677.
29. Belloni PN, Garvin L, Mao CP, Bailey-Healy I, Leaffer D. Effects of all-trans-retinoic acid in promoting alveolar repair. *Chest* 2000;117:235S–241S.
30. Barnes PJ, Hansel TT. Prospects for new drugs for chronic obstructive pulmonary disease. *Lancet* 2004;364:985–996.